Polarization dynamics in the mixed ferroelectric $KTa_{1-x}Nb_xO_3$

L. A. Knauss, R. Pattnaik, and J. Toulouse
Physics Department, Lehigh University, Bethlehem, Pennsylvania 18015
(Received 14 May 1996; revised manuscript received 19 September 1996)

Mixed ferroelectrics exhibit unusual precursor effects. In $KTa_{1-x}Nb_xO_3$, polar nanoregions have been shown to condense approximately 20 K above the transition for all Nb concentrations, $1.2\%<x<50\%$, as a result of medium-range collective interactions between Nb off-center ions. These interactions are also responsible for the observation of hysteresis loops in the polarization and dielectric nonlinearities far above the transition. In the present study we have identified three distinct polarization regimes: (1) dynamic and (2) quasistatic, both above the transition, and (3) static, below the transition. The first two regimes can be distinguished by the shape of the hysteresis loops, changing from oval to *s* shape, and by their frequency dependence. We have analyzed the harmonic content of the polarization response and show that the condensation of polar nanoregions coincide with the appearance of odd harmonics which are indicative of a nonlinear response. This is further supported by the observation of a nonlinear dielectric response that becomes progressively stronger with decreasing temperature below the condensation. We also show that there exists a direct relationship between dielectric and polarization response and that one can be calculated from the other. Finally, the low-frequency dynamics exhibited in the quasistatic range can be qualitatively explained by the strong interaction between neighboring off-center Nb ions within polar nanoregions and random interactions between these regions. [S0163-1829(97)07105-1]

I. INTRODUCTION

Ferroelectric transitions are normally marked by a maximum in the dielectric constant and the appearance of a spontaneous or remanent polarization. This is, for example, the case in $KNbO_3$ which undergoes a first-order ferroelectric transition at 708 K.[1] The behavior of mixed ferroelectrics can be very different and particularly so when the mixed or substituted ions are randomly distributed and in off-center positions. Because they are off center, these ions form dipole moments in what can therefore be called *random dipole ferroelectrics*. It is already well known that some of them exhibit slow relaxations and are consequently identified as *relaxors*.[2] $K_{1-x}Li_xTaO_3$ (KLT) was recently shown to be a typical example of this group, in which the relaxor behavior is due to the randomly distributed off-center Li ions.[3] In the present paper we report on a polarization study of a related system, $KTa_{1-x}Nb_xO_3$ (KTN), with off-center Nb ions,[4] which presents a distinctly different kind of polarization behavior.

Both KLT and KTN are derived from the same parent system, $KTaO_3$, which is an ''incipient ferroelectric,'' i.e., one that, even though it possesses a definite soft mode, does not transform. The substitution of Li for K or Nb for Ta, in excess of 2.2% (Ref. 5) and 0.8% (Ref. 6), respectively, induces a transition. However, the two systems are different in several respects. In particular, because of the deeper potential well or the greater local distortion around Li (Ref. 7) than around Nb,[8] KLT is much less polarizable than KTN. This probably also explains why at high temperature, KTN retains the cubic perovskite structure for all values of x while KLT goes into $LiTaO_3$ which has a distorted perovskite structure.[9]

A particular feature of the two mixed systems KLT and KTN is the formation of polar nanoregions well above the transition. These have been evidenced through polarization,[10] Raman scattering,[11,12] ultrasonic,[13] and NMR (Ref. 14) measurements. However, both the formation mechanism and the collective dynamics of these polar nanoregions are very different in KLT and KTN. It was recently shown that, while in KLT these regions appear at the same high temperature ($\sim$200 K) for all Li concentrations,[15] in KTN they appear approximately 20 K above the actual ferroelectric transition for all Nb concentrations, pointing to a cooperative phenomenon (condensation).[16] It is important to note, however, that the transition temperature, T_c, itself does depend on concentration. The presence of polar nanoregions above T_c in strongly polarizable KTN necessarily modifies the character of the phase transition which can no longer be simply displacive. In the present paper, we report the results of a detailed investigation of the polarization dynamics over a range of niobium concentrations. In Sec. II we briefly describe the experimental setup used to measure the polarization hysteresis loops. Section III examines successively their temperature and their frequency dependencies. Results of dielectric constant measurements under dc bias fields are also presented in order to evaluate the dielectric nonlinearities and complement the polarization results. Section IV presents an analysis of the polarization results which distinguishes between a purely dynamic and a quasistatic behavior and establishes a connection between polarization and dielectric nonlinearities.

II. EXPERIMENT

The polarization dynamics were studied in several KTN crystals grown at Oak Ridge National Laboratory with different Nb concentrations ($x=1.2\%,3\%,15.7\%$). All the samples were slabs with approximate dimensions $0.4\times0.4\times0.06$ cm and with Al electrodes evaporated on the two main faces. The oscillating fields were derived from a signal

generator, the output of which was amplified through a bipolar amplifier and applied across the sample. The measurements were made using a Sawyer-Tower circuit,[17] the voltage across the reference capacitor being fed to a digital oscilloscope. The full hysteresis loops were directly transferred to the computer for analysis. Fields up to 2 kV/cm were applied at frequencies between 100 Hz and 1 kHz. Measurements were made as a function of increasing temperature, allowing the samples to equilibrate for 15 min at each temperature before measurement.

In order to determine the most relevant range of temperatures to be studied ($T_c \rightarrow T_c + 20$ K), the transition temperature, T_c, was determined from the peak of the dielectric constant. For the three concentrations investigated, the transition temperatures were found[16] to be 12.2 K (1.2%), 59.5 K (3%), and 138.8 K (15.7%.)

III. RESULTS

The two principal quantities obtained from hysteresis loops are the maximum polarization, $P_{\max}$, corresponding to the maximum field and the remanent polarization, P_r, corresponding to zero field. In conventional (pure) ferroelectrics, for temperatures above the transition, $P_r = 0$ and P is usually linear in the field:

$$P = \chi E, \tag{1}$$

where χ is the dielectric susceptibility. As mentioned in the Introduction, in the mixed ferroelectric KTN, hysteresis loops are observed well above T_c and their shape changes at approximately $T_c + 20$ K.

A. Temperature dependence of hysteresis loops

Figure 1 shows hysteresis loops for all three concentrations at temperatures both above and below T_c measured at a frequency of 40 Hz. One can distinguish three separate ranges: far above the transition ($> T_c + 20$ K) the system exhibits a typical linear dielectric behavior and oval loops are observed (see also Fig. 5); as the transition is approached ($T_c < T < T_c + 20$ K), the loops open up and take on a typical *s* shape with a finite P_r, due to the presence of polar regions; below the transition ($T < T_c$), the loops become more square, with P_r approaching $P_{\max}$, which indicates that the system is truly ferroelectric.

P_r, $P_{\max}$, and the area inside the loop increase with Nb concentration, pointing to the essential role of niobium in the formation of the polar nanoregions. Nevertheless, the evolution of the shape of the loops with temperature is basically the same for all three concentrations investigated, suggesting similar polarization dynamics for all of them. Consequently, we use the polarization results obtained with the middle concentration (3%) for the following discussion.

B. Frequency dependence of hysteresis loops

The frequency dependence of the hysteresis loops, and more specifically of their shapes, yields significant information on the dynamics of polarization. In Fig. 2 a set of loops is presented for KTN 3% in each of the three temperature ranges identified above.

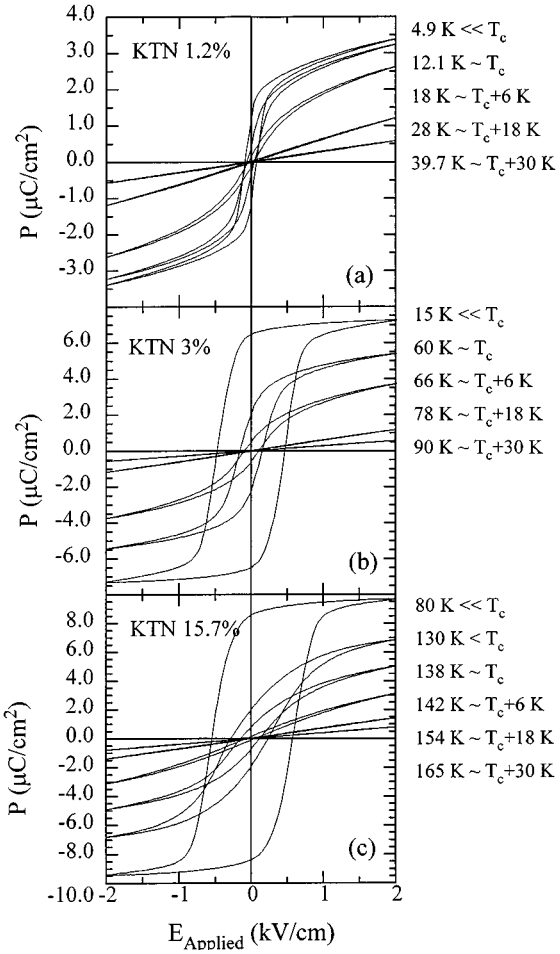

FIG. 1. The 40 Hz hysteresis loops of KTN (a) 1.2%, (b) 3%, and (c) 15.7% at various temperatures. The temperatures listed on the right side of the graph correspond to the hysteresis loops in the order of their maximum polarization.

Figure 2(a) shows that, in the purely dynamic range ($T_c + 30$ K), the loops can be slightly opened and oval at high enough frequencies, but disappear at low frequencies. In the intermediate or quasistatic range ($T_c + 8$ K), the loops exhibit an *s*-shape (slim loops) which is also strongly frequency dependent. In this range, the frequency dependence can be characterized by noting that $P_{\max}$ decreases while P_r increases with frequency. In contrast, below the transition, both $P_{\max}$ and P_r decrease with increasing frequencies, and the loops are much more square.

A summary of $P_{\max}$ and P_r is presented in Fig. 3 as a function of temperature and for several frequencies between 10 and 1000 Hz. Both $P_{\max}$ and P_r increase with concentration, with $P_{\max}$ roughly proportional to the Nb concentration. Figure 3(b) also further illustrates the crossover in the frequency dependence which occurs near the transition; above T_c, P_r increases with increasing frequency while, below T_c, the tendency is reversed and P_r decreases (as it normally should behave) with increasing frequency.

C. Dielectric constant under dc bias fields

In order to complement the polarization measurements using the hysteresis loop method, we have also carried out dielectric constant measurements under a dc bias field. In

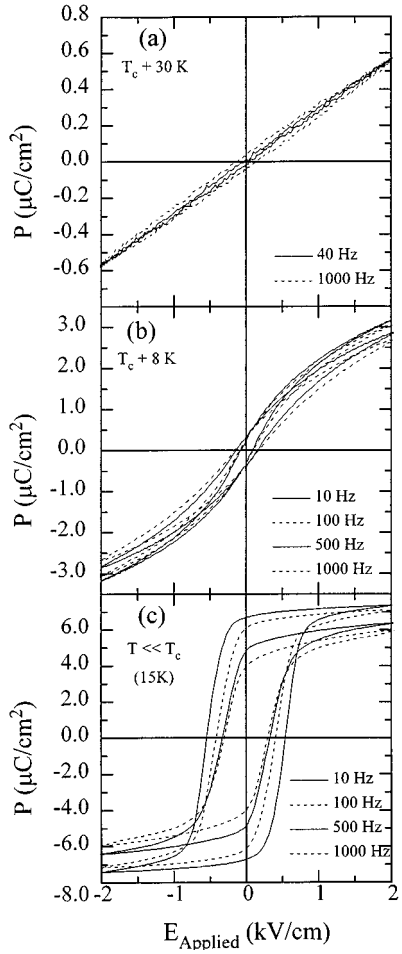

FIG. 2. Hysteresis loops of KTN 3% measured at several frequencies for temperatures (a) T_c+30 K, (b) T_c+8 K, and (c) $T \ll T_c$. The frequencies listed on the right side of the graph correspond to the hysteresis loops in the order of their maximum polarization.

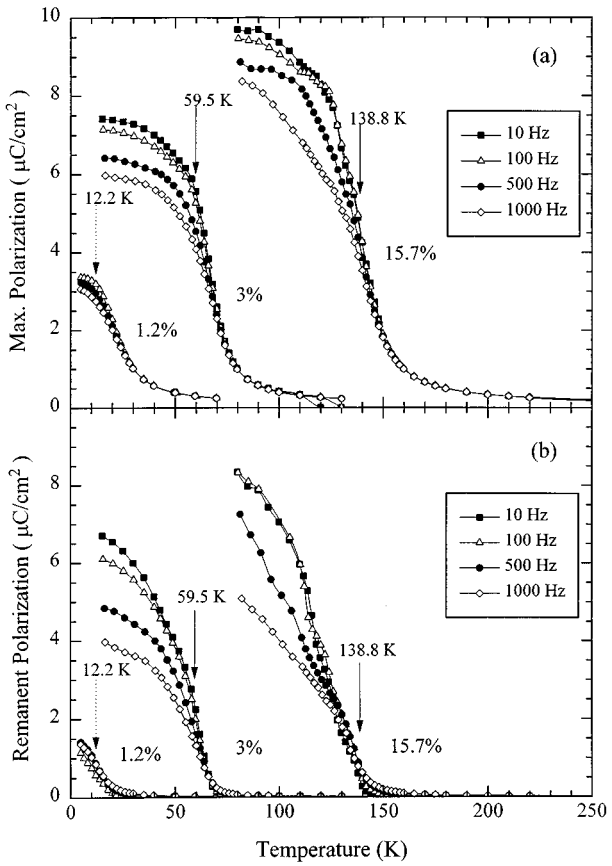

FIG. 3. (a) Maximum polarization and (b) remanent polarization for each concentration of KTN measured at frequencies ranging from 10 to 1000 Hz. The arrows indicate the temperature of the maximum dielectric susceptibility for each concentration.

fact, $P_{\max}$ obtained from hysteresis loops in the high-field (saturation) limit should be comparable with P_{ind} induced by the dc bias field calculated from the dielectric constant measurements. Moreover, there should exist a connection between polarization and dielectric nonlinearities.

The dielectric results are presented in Fig. 4. At high temperature, all curves follow a Curie-Weiss law, $\varepsilon^{-1} \sim (T - T_0)$, with a field-dependent slope (see the inset in Fig. 4), a point that will be discussed in a later and more specialized publication. At low temperature, the dc bias field strongly suppresses the dielectric susceptibility, particularly so below 160 K (T_c+20 K). This latter observation further highlights the importance of the contribution of polar regions to the zero-field susceptibility. Finally we note that, under a dc bias field, the cubic tetragonal transition shifts to higher temperatures while the tetragonal-orthorhombic transition shifts to lower temperatures. The tetragonal phase is therefore stabilized by strains resulting from an electrostrictive or a field-induced piezoelectric effect.

IV. ANALYSIS

A careful examination of the results reveals the existence of two distinct regimes in the polarization behavior above the transition. At higher temperature ($T > T_c+20$ K), the polarization is purely dynamic and can be associated with entropy fluctuations characterized by a lifetime. With the appearance of polar nanoregions, the polarization becomes quasistatic and exhibits orientational dynamics characterized by a jump frequency or a reorientation time and both the polarization and dielectric constant exhibit nonlinearities.

A. Pure dynamic range

Far above the transition ($T > T_c+20$ K), KTN behaves as a linear dielectric of an unusual type, with very large dynamical polar fluctuations. As shown in Fig. 2(a) and in Fig. 5, hysteresis loops are observed that are oval in shape. The linear character of the polarization in this range is demonstrated in Figs. 5(b) and 5(c) which show that the maximum polarization, $P_{\max}$, is strictly proportional to the maximum amplitude of the field, E_0 (respectively, 2 and 1 kV/cm). The dynamic character of the polarization in this range is demonstrated by the change of the area inside the loops with frequency; as the frequency decreases, the loops become narrower so that the remanent polarization tends to vanish. The decreasing width of the loops with frequency proves that the remanent polarization observed is purely dynamical in nature and that there is no spontaneous polarization in this range: $P_r(\Omega=0)=0$.

The oval shape of the loop is indicative of a phase lag between the applied field and the polarization response as

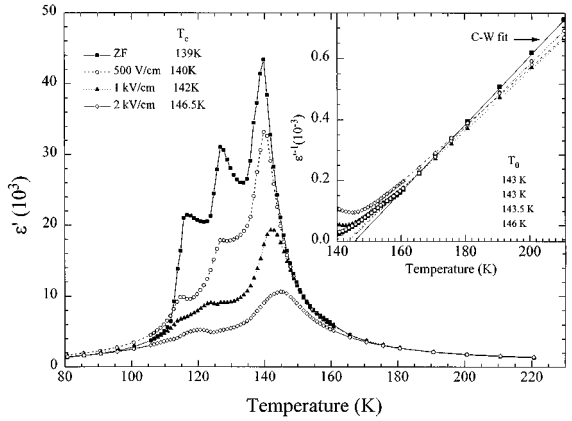

FIG. 4. Real dielectric constant of KTN 15.7% as a function of temperature for different dc bias fields. T_c is the actual transition temperature. T_0 is the Curie-Weiss temperature.

can be confirmed by a comparison with dielectric results. Indeed, the existence of a phase lag implies that the polarization contains an imaginary as well as a real component and can therefore be written as

$$P=(\varepsilon'\cos\Omega t+\varepsilon''\sin\Omega t)\varepsilon_0 E_0\,, \tag{2}$$

where ε' and ε'' represent the real and imaginary parts of the dielectric constant, ε_0 is the permittivity of free space, E_0 the maximum amplitude of the applied ac electric field, and Ω its frequency. Figure 5 shows that Eq. (2) can be fitted quite satisfactorily to the hysteresis loops. The fitted values of ε' and ε'' are given in Table I along with the values obtained from the direct ac dielectric measurements reported above under a dc bias field. The values of ε' obtained from fitting the hysteresis loops are close to the directly measured values, confirming that, in this temperature range, the dielectric response is mostly linear. In the case of ε'', the much larger values obtained from fitting the hysteresis loops are indicative of the strong effect of the field on the lifetime of the polarization fluctuations and on the resulting phase lag. The relationship between hysteresis loops and dielectric measurements is discussed later in the paper.

B. Quasistatic range

As mentioned in the Introduction, it has recently been shown that, for all concentrations of KTN between 1.2 and 30%, long-lived polar nanoregions condense at approximately T_c+20 K. The present polarization results show that the condensation of these polar regions is accompanied by a change in the shape of the hysteresis loops from oval to *s*-shape, thereby displaying saturation effects and a nonlinear dependence of the polarization on the applied ac field.

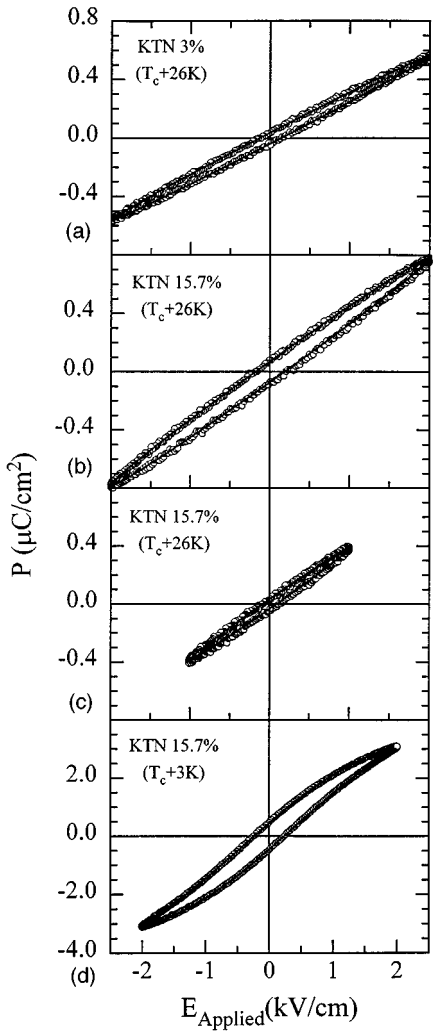

FIG. 5. Hysteresis loops at $T>T_c+20$ K from KTN (a) 3%, (b) 15.7% for $E_0=2$ kV/cm, (c) 15.7% for $E_0=1$ kV/cm, and (d) at $T_c<T<T_c+20$ K from KTN 15.7% for $E_0=2$ kV/cm. The solid lines are fits of the polarization with Eq. (2) (a)–(c) and Eq. (3) (d).

TABLE I. Comparison of dielectric constants obtained from fitting the polarization hysteresis loops and from direct dielectric measurements. The asterisk means the measured values for the 3% were obtained in zero field.

		ε'		ε''	
Conc. (X)	Field (E_0)	Dielectric meas.	Polarization Fit	Dielectric meas.	Polarization Fit
$T=T_c+26$ K					
3%	2 kV/cm	3 411*	3 168	26*	217
15.7%	2 kV/cm	4 218	4 394	16	406
15.7%	1 kV/cm	4 580	4 322	36	390
$T=T_c+3$ K					
15.7%	2 kV/cm	10 099	21 755	51	2609

In this quasistatic range, the polarization can be well described by a more general expression:[18]

$$P = c\ \tanh(aE_0\cos\Omega t + bE_0\sin\Omega t). \tag{3}$$

We note that the hyperbolic tangent is obtained when calculating the average polarization of an Ising system. This is therefore an expression that one would naturally construct to describe the dynamics of an Ising system in which the polarization response lags behind the applied field, due to the interactions between dipoles. A similar model has been used by Bell[19] to analyze the superparaelectric behavior of relaxors. The fit of this expression to the *s*-shape hysteresis loops is almost perfect as illustrated in Fig. 5(c). The extraction of ε' and ε'' values from the fitted values of the parameters is slightly more difficult than in the previous linear case but can be obtained by taking the derivative dP/dE_0 in the limit $E_0 \to 0$:

$$\frac{dP}{dE_0} = c[\mathrm{sech}(aE_0\cos\Omega t + bE_0\sin\Omega t)]^2 \times [a_0\cos\Omega t + b\ \sin\Omega t], \tag{4}$$

$$\varepsilon_0\varepsilon^* = \left.\frac{dP}{dE_0}\right|_{E_0\to 0} = ca\cos\Omega t + cb\ \sin\Omega t \tag{5}$$

such that

$$\varepsilon_0\varepsilon' = ca \quad \text{and} \quad \varepsilon_0\varepsilon'' = cb. \tag{6}$$

The values of ε' and ε'' thus obtained from the fit of the hysteresis loops are listed in Table I along with the values obtained from direct ac dielectric measurements. The fitted values are again higher than the measured ones, but more so now in the quasistatic range than previously in the dynamic range. This is particularly significant for ε' but should be expected because of the much larger field applied in the hysteresis loop measurements. In these measurements, the large ac field can switch the polar regions which therefore contribute a significant amount to ε', while in the direct dielectric measurements, the switching of the polar regions is impeded by the presence of the large dc bias field.

The nonlinear character of the polarization in the quasistatic range is clearly shown by the hyperbolic tangent form of the polarization, but it appears even more explicitly in a Fourier analysis of the polarization signal:

$$P = \chi^{(1)}(\Omega)E - \chi^{(2)}(2\Omega)E^2 + \chi^{(3)}(3\Omega)E^3 - \cdots . \tag{7}$$

It is important to note that the second harmonic of the polarization, being proportional to E^2, contributes an E^3 (odd) term to the energy and can only be present if the macroscopic inversion symmetry is broken. The results of the Fourier analysis of the polarization signal are shown in Fig. 6 for KTN 3% and 15.7% measured upon heating. The most important feature on this figure is the rise of the third harmonic below $T_c + 20$ K for both concentrations, even though their respective transition temperatures, T_c, are very different. *This clearly points to the polar nanoregions as the cause of the polarization nonlinearities*. It is worth noting that, while the magnitude of the third harmonic decreases with increasing fundamental frequency, the temperature dependence is approximately the same at all frequencies. This is shown in the inset of Fig. 6, where the third harmonic curves have all been normalized to one at the lowest temperature.

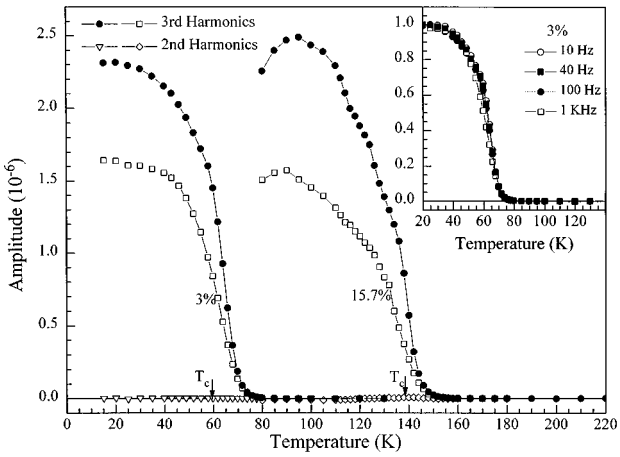

FIG. 6. Amplitude of the third and second harmonics obtained from Fourier analysis of the polarization signal. ●, 100 Hz excitation; □, 1 KHz excitation. Inset: The normalized third harmonic amplitude for different excitation frequencies as given in the legend.

The third harmonic in the cubic phase can only be due to electrostriction and it gives rise, in the low symmetry phase, to an induced piezoelectric effect.[20] In contrast to the third harmonic, the second harmonic remains negligibly small at all temperatures. This observation is understandable above T_c, since the macroscopic inversion symmetry does not allow for even powers of the field to appear in the polarization. However, in the low-symmetry phase, the second harmonic will only be zero if the polarization is completely switched by the oscillating field or if the crystal is multidomain. In KTN, the relatively large polarization supports the first explanation and indicates that KTN is an unusual soft polar ferroelectric.

C. Field-induced polarization and nonlinearity

As shown earlier, the dielectric constant, real and imaginary parts, could be obtained from the hysteresis loops. However, because the two types of measurements were not made under the same conditions, a large ac field in one case and a large dc field in the other, we found discrepancies between the fitted values of the dielectric constant and the directly measured ones. In this section we analyze the origin of these discrepancies. A similar nonlinear dielectric measurement on doped $SrTiO_3$ and $KTaO_3$ has been reported by Dec *et al.*[21] and Maglione *et al.*[22]

When a dc bias field, E_0, is applied to the sample, inversion symmetry is broken and a finite polarization, P_{ind}, is induced, which can be calculated from the experimental dielectric data. P_{ind} can then be compared to the maximum polarization, $P_{\max}(\Omega, E_0)$, measured on the hysteresis loops. However, as we mentioned above, there exists an important difference between hysteresis loops and nonlinear dielectric measurements which is that, in the former, the macroscopic polarization is time varying while, in the later, it is time

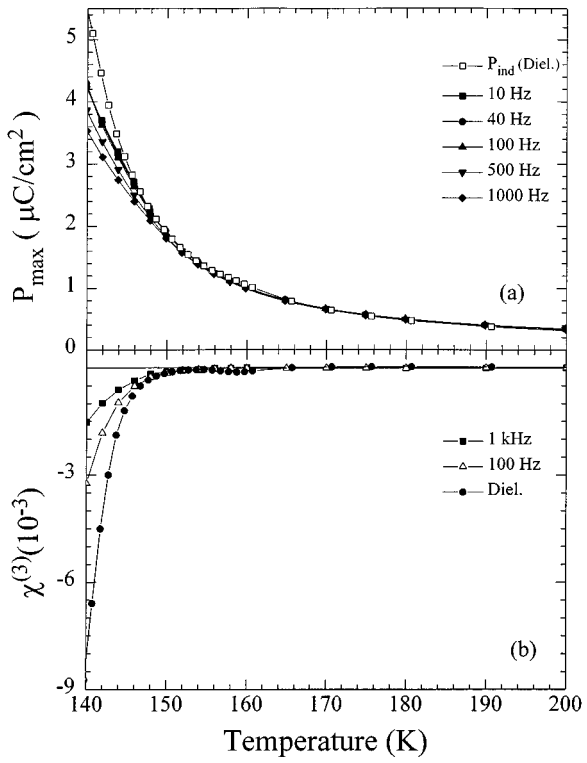

FIG. 7. (a) dc field induced polarization ($P_{\rm ind}$), and maximum polarization ($P_{\rm max}$) from hysteresis loops (at different frequencies) for KTN 15.7% with $E_{\rm max}=2$ kV/cm. (b) $\chi^{(3)}$ derived from the data of the third harmonic polarization, and nonlinear dielectric constant (Diel).

independent. For this reason, the comparison is only valid in the limit of zero-frequency hysteresis loop measurements, $P_{\rm max}(0,E_0)$.

The induced polarization, $P_{\rm ind}$, can be calculated from experimental dielectric data by first writing the total polarization in the presence of a dc bias field as

$$P(\omega,E_0)=\chi^{(1)}(\omega)[E_0+e_0\sin\omega t] + \chi^{(3)}(\omega)[E_0+e_0\sin\omega t]^3$$

in which we only keep the lowest-order nonlinear term, and e_0 and ω are, respectively, the magnitude and frequency of the small signal ac probe field. We note that $\chi^{(3)}$ from the dielectric measurements was estimated at the fundamental frequency ω. We then expand the right-hand side of the above equation, neglecting e_0^2 and e_0^3 terms, to obtain:

$$\begin{aligned}P(\omega,E_0)&=\chi^{(1)}(\omega)E_0+\chi^{(3)}(\omega)E_0^3 \\ &\quad+[\chi^{(1)}(\omega)+\chi^{(3)}(\omega)E_0^2]e_0\sin\omega t \\ &=P_{\rm ind}(E_0)+\chi(\omega,E_0)e_0\sin\omega t,\end{aligned}$$

where the last expression defines $P_{\rm ind}(E_0)$ which can be estimated from the experimentally measured dielectric quantities, $\chi^{(1)}(\omega)=\chi(\omega,0)$ and $\chi(\omega,E_0)$. $P_{\rm ind}$ is compared to $P_{\rm max}$ in Fig. 7(a). The two quantities are equal at high temperatures but $P_{\rm max}(\Omega,E_0)$ is found to be lower than $P_{\rm ind}(E_0)$ at low temperatures (below the condensation temperature) but tending towards $P_{\rm ind}$ in the limit $\Omega=0$.

Similar remarks apply to the comparison between $\chi^{(3)}$ results from hysteresis loop and dielectric measurements. In the dielectric case, the measured $\chi^{(1)}(\omega)$ and $\chi(\omega,E_0)$ can be used to estimate $\chi^{(3)}(\omega)$, which can then be compared with $\chi^{(3)}(3\Omega)$ determined from the third harmonic polarization signal. To determine $\chi^{(3)}(3\Omega)$ from the hysteresis loop measurements, we assume an excitation of the form $E(t)=E_0\sin\Omega t$ in Eq. (7). Retaining only the first nonlinear coefficient, it can then be shown that

$$\chi^{(1)}(\Omega)+\frac{3}{4}E_0^2\chi^{(3)}(3\Omega)=\frac{\Omega}{\pi E_0}P_\Omega$$

and

$$\chi^{(3)}(3\Omega)=\frac{4\Omega}{\pi E_0^3}P_{3\Omega}, \tag{8}$$

where

$$P_{n\Omega}=\int_0^T dt\,P(t)\sin n\Omega t, \quad n=1,2,3,\ldots .$$

Here $P(t)$ is the measured polarization signal, $T=2\pi/\Omega$ is the period, and $P_{n\Omega}$ is the amplitude of the nth harmonic present in the measured signal (see Fig. 6). The $\chi^{(3)}$ curves determined from the dielectric and hysteresis loop measurements are presented in Fig. 7(b). In the high-temperature region $\chi^{(3)}$ and $\chi^{(3)}(3\Omega)$ are small but almost equal to each other.

Below the condensation, $\chi^{(3)}(3\Omega)$ is seen to be frequency dependent, but tending towards $\chi^{(3)}$ in the limit of $\Omega=0$. We have thus established the relationship that exists between hysteresis loop measurements and the dielectric measurements under a dc bias field.

It is important to note that, in the dielectric measurements under a dc field, the system is in equilibrium and the induced polarization is maximum while, in the hysteresis measurements the system is not in equilibrium and the magnitude of the induced polarization depends on the frequency. It can then be concluded that the $\chi^{(3)}$ obtained from the nonlinear dielectric measurements is the maximum attainable first nonlinear coefficient and $P_{\rm ind}$ the maximum attainable polarization.

D. Ferroelectric range

A set of hysteresis loops, measured at different frequencies and well below T_c, is shown in Fig. 2(c). The loops have a much squarer shape than in Fig. 2(b), suggesting the existence of a static and stable polarization. This is further confirmed by the frequency dependence of the loops which, in this range, is opposite to what it is at higher temperature; namely, both $P_{\rm max}$ and P_r now increase with decreasing frequency, thus showing that the polarization induced by the external field is retained after removal of the field.

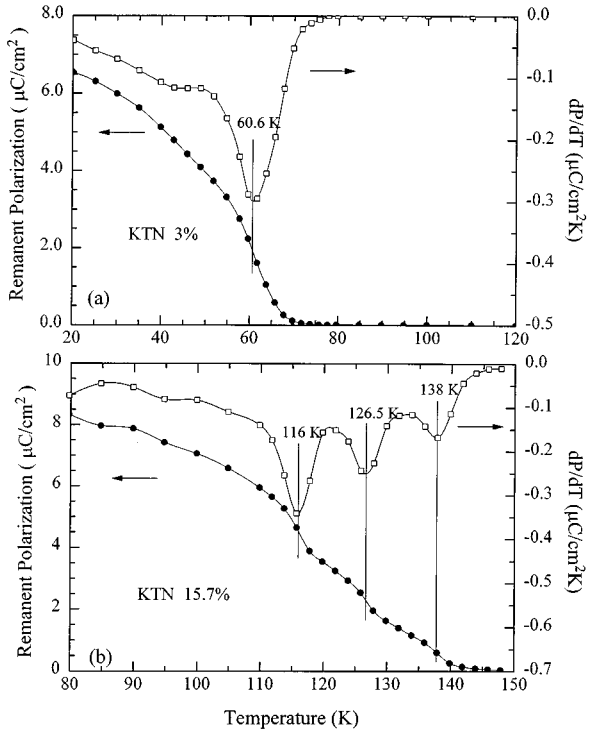

FIG. 8. Remanent polarization and its temperature derivative for KTN (a) 3% and (b) 15.7%. The inflection points of the remanent polarization match the peak of the dielectric constant.

E. Phase transitions

The final observation of this study concerns the determination of the phase transition, based upon measurements of the remanent polarization, P_r. Figure 8 shows P_r vs T as well as the derivative dP_r/dT for both the 3% and the 15.7% KTN crystals. The inflection points in the P_r curves are found to coincide with the transition temperatures determined from the maxima of the dielectric constant.[16] In fact, this observation even suggests the existence, in KTN 3%, of at least one lower transition around 45 K which is not resolved in the dielectric measurements. This would confirm a recent ultrasonic study[13] that showed that, for lower concentrations of niobium, three phase transitions are still occurring which are too close to one another to be resolved but can be separated (or possibly induced) by the application of a dc bias field.

F. Model of polarization dynamics

The slow polarization dynamics that we have reported above in the quasistatic range cannot be understood in terms of the simple reorientation of individual Nb off-center ions. The frequency of such a reorientation was estimated earlier and shown to follow an Arrhenius relation at high temperature:[23]

$$\nu = \nu_0 \exp(-U_d/T), \tag{9}$$

with the activation energy $U_d = 70$ K and the preexponential $\nu_0 = 300$ cm^{-1}. The reorientation frequencies corresponding to this relation are in the terahertz range and therefore much higher than the frequencies of the present polarization measurements. Consequently, the low-frequency polarization dynamics observed in the present work must be due to interacting off-center Nb ions. A few years ago, a model was developed to describe the low-frequency kinetics in random-site electric dipole systems.[3,18] In this model, the interactions between neighbor dipoles were treated exactly to describe the dynamics of pairs. The reorientation of strongly interacting dipoles in pairs, was shown to take place at a much lower frequency than the noninteracting dipoles:

$$\nu = \nu_0 \exp\left(-\frac{U_d + U_{dd}}{T}\right)$$

in which U_{dd} is the additional energy barrier due to the strong interaction in pairs. An explicit expression for U_{dd} has been derived and discussed in Ref. 16. Using this model, separate calculations of the polarization and the dielectric constant were performed.[18] In particular, it was found that the polarization could be approximated by an expression similar to Eq. (3) above.

V. CONCLUSION

Our earlier experiments have unambiguously revealed the presence of groups of strongly interacting dipoles in what has been named polar nanoregions.[16] We have shown that, in KTN, these polar nanoregions appear at $T^*(n) \cong T_c(n) + 20$ K for all concentrations n. The present KTN study of hysteresis loops and dielectric constant under a dc bias field reveals that the onset of polarization and dielectric nonlinearities coincide with the condensation of these polar regions. This condensation thus marks a crossover from a purely dynamic regime to a quasistatic one. In the purely dynamic regime, the polarization and dielectric responses are linear. The hysteresis loops are oval in shape, the remnant polarization is strictly due to the phase lag between the polarization response and the applied field. In the quasistatic regime the polarization and dielectric responses become nonlinear. The polarization response contains odd harmonics and the dielectric nonlinearities depend more weakly on temperature. In the quasistatic regime, we have also shown that the results from polarization hysteresis loop measurements are identical to the nonlinear dielectric measurements in the limit of zero frequency. *These results clearly identify the randomly distributed polar regions in the strongly polarizable lattice as the source of the nonlinear dynamical properties in KTN above* T_c. Similar polar regions may also be the source of slow dynamics, nonlinear dielectric and polarization properties in other mixed-disordered ferroelectrics.

ACKNOWLEDGMENTS

Special thanks are due to L. A. Boatner for the growth of excellent single crystals. This work was supported by the U.S. Department of Energy under Grant No. DE-FG02-86ER45258 (L.A.K.) and by the Office of Naval Research under Grant No. N00014-90-J-4098 (R.P.).

[1] M. D. Fontana, G. Metrat, J. L. Servoin, and F. Gervais, J. Phys. C **16**, 483 (1984); A. W. Hewat, *ibid*. **6**, 2559 (1973).
[2] N. Setter and L. E. Cross, J. Appl. Phys. **51**, 4356 (1980); Phys. Status Solidi A **61**, K71 (1980).
[3] J. Toulouse, B. E. Vugmeister, and R. Pattnaik, Phys. Rev. Lett. **73**, 3467 (1994).
[4] O. Hanske-Petitpierre, Y. Yacoby, J. Mustre de Leon, E. A. Stern, and J. J. Rehr, Phys. Rev. B **44**, 6700 (1991).
[5] W. Kleemann, S. Kutz, F. J. Schafer, and D. Rytz, Phys. Rev. B **37**, 5856 (1988).
[6] U. T. Hochli, H. E. Weibel, and L. A. Boatner, Phys. Rev. Lett. **39**, 1158 (1977).
[7] F. Borsa, U. T. Hochli, J. J. Van Der Klink, and D. Rytz, Phys. Rev. Lett. **45**, 1884 (1980).
[8] K. B. Lyons, P. Fleury, and D. Rytz, Phys. Rev. Lett. **57**, 2207 (1986).
[9] S. C. Abrahams and J. L. Bernstein, J. Phys. Chem. Solids **28**, 1685 (1967).
[10] J. Toulouse, X. M. Wang, L. A. Knauss, and L. A. Boatner, Phys. Rev. B **43**, 8297 (1991).
[11] J. Toulouse, P. DiAntonio, B. E. Vugmeister, X. M. Wang, and L. A. Knauss, Phys. Rev. Lett. **68**, 232 (1992).
[12] P. DiAntonio, B. E. Vugmeister, J. Toulouse, and L. A. Boatner, Phys. Rev. B **47**, 5629 (1993).
[13] L. A. Knauss, X. M. Wang, and J. Toulouse, Phys. Rev. B **52**, 13 261 (1995).
[14] J. J. van der Klink, S. Rod, and A. Châtelain, Phys. Rev. B **33**, 2084 (1986); S. Rod and J. J. van der Klink, *ibid*. **49**, 470 (1994).
[15] P. DiAntonio, J. Toulouse, B. E. Vugmeister, and S. Pilzer, Ferroelectrics Lett. **17**, 115 (1994).
[16] J. Toulouse and R. K. Pattnaik, J. Phys. Chem. Solids (to be published).
[17] C. B. Sawyer and C. H. Tower, Phys. Rev. **35**, 269 (1930).
[18] B. E. Vugmeister and P. Adikhari, Ferroelectrics **157**, 2625 (1994).
[19] A. J. Bell, J. Phys. Condens. Matter **5**, 8773 (1993).
[20] F. Jona and G. Shirane, *Ferroelectric Crystals* (Dover, New York, 1993), pp. 75 and 147.
[21] J. Dec *et al.*, Europhys. Lett. **29**, 31 (1995).
[22] M. Maglione, M. Lopes Dos Santos, M. R. Chaaves, and A. Almeida, Phys. Status Solidi B **181**, 73 (1994); M. Maglione, U. T. Höchli, and J. Joffin, Phys. Rev. Lett. **57**, 436 (1986).
[23] H. Uwe, K. B. Lyons, H. L. Crater, and P. Fleury, Phys. Rev. B **33**, 6436 (1986).